# Doping dependence of high-energy spectral weights for the high-$T_c$ cuprates

H. Eskes and G. A. Sawatzky
*Materials Science Centre, Department of Solid State and Applied Physics, University of Groningen, Nijenborgh 18, 9747 AG Groningen, The Netherlands*
(Received 14 June 1990)

In this paper we present calculations of the photo- and inverse photoemission spectra, and the O 1*s* and Cu 2*p* core-level spectra for the high-$T_c$ materials, using a multiband Hubbard Hamiltonian. The spectra are obtained for small clusters containing two Cu atoms ($Cu_2O_7$ and $Cu_2O_8$) for the undoped, electron-doped, and hole-doped cases. In order to investigate the sensitivity of the spectra to cluster size and localized versus delocalized oxygen levels, a comparison is made with a (**k**-dependent) impurity approach and results from a $CuO_4$ cluster. Special attention is paid to the doping dependence of the spectra and the low-energy states and to the redistribution of spectral weights upon doping.

## INTRODUCTION

In spite of the large amount of work dedicated to the high-$T_c$ superconductors, one can say that their electronic structure is still not well understood.[1] The problem originates from the fact that we are dealing with covalent materials with strong correlations.[2] The covalency is clearly illustrated by the large value of Cu-O hopping or transfer-matrix elements. Furthermore, this covalent nature is not restricted to only one orbital per site (like the often-chosen $d_{x^2-y^2}$ for copper and $p_\sigma$ for oxygen), but there is a direct mixing of most of the Cu 3*d* and O 2*p* states. The biggest problem however is the large Coulomb repulsion between holes on the copper. Estimates show that these interactions ($U \simeq 8-9$ eV) are larger than or at least of the order of the total width of the combined Cu-O band and have to be taken into account explicitly in a realistic calculation.

That we are dealing here with a complicated many-body problem is also evidenced by local-density-approximation (LDA) band-structure calculations which are now available for most of the high-$T_c$ compounds.[3] These calculations play an important role in identifying the essential orbitals and determining tight-binding parameter values.[4–7] However, interpreting the one-particle eigenvalues resulting from the ground-state calculation as being excitations of the system has led to poor results. In the first place the standard LDA calculation predicts no energy gap at the Fermi level for the antiferromagnetic "undoped" compounds, while this gap is known to be 1.5–2 eV.[8] Furthermore, the LDA ground-state calculations predict states in the energy region from $E_F$ to only about 7 eV binding energy, while in this photoemission spectra (PES) a large signal is seen up to 16 eV with a large and broad structure around 12–13 eV below the Fermi level. This appearance of a high-energy signal is a well-known characteristic of highly correlated systems.

Photoemission and inverse photoemission spectroscopy (IPES or BIS) are important tools in unraveling the electronic structure of these compounds. In a one-particle picture, these experiments give (in principle) directly the occupied and unoccupied (partial) density of states, and in a correlated many-particle framework the spectral distribution is a direct measurement of the one-electron many-body Green's function.

One of the first interpretations of the photoemission spectra for the high-$T_c$ compounds in terms of a many-body configuration interaction was given by Shen *et al.*[9] They obtained rough estimates of the Cu Coulomb interaction $U$, the charge transfer energy $\Delta$, and the Cu-O hybridization by considering a $3\times3$ matrix problem for the final state containing the configurations $d^8$, $d^9\underline{L}$, and $d^{10}\underline{L}$. Later, more involved calculations in the same spirit have been done for small clusters ($CuO_{4,5,6}$),[10–12] or using an impurity approach.[5,13–15]

In order to obtain a good description of experiments, a few considerations are of importance. In the first place, *all* Cu 3*d* and O 2*p* states have to be included. Many-body one-hole Green's functions have been calculated numerically by some groups[16,17] for a small cluster ($Cu_4O_8$) or with a slave-boson approach,[18,19] using $d_{x^2-y^2}$ and $p_\sigma$ orbitals only . These electron-removal Green's functions cannot directly be related to PES experiments, because only about 15% of the total *d*-spectral weight comes from the $d_{x^2-y^2}$ orbital. In Fig. 1 we show the combined x-ray photoemission spectroscopy (XPS) and BIS spectrum for this reduced basis set for the $Cu_2O_7$ cluster. Clearly, the overall shape is quite different from the one observed in XPS or from calculations including the full set of orbitals, as we will show below. Second, Cu $d^8$ has a rich atomic Coulomb and exchange multiplet structure with energy values distributed over a range of about 7 eV.[12,13] This splitting of levels is seen very clearly in Auger data for metallic copper.[20,21] In Fig. 1, where only the $d_{x^2-y^2}$ orbital is involved, this multiplet structure is completely lost, and the $d^8$ part of the spectrum shows a single sharp peak at about 14 eV.

Of course, taking a full basis set seriously restricts the size of the cluster one is able to compute. In the

 

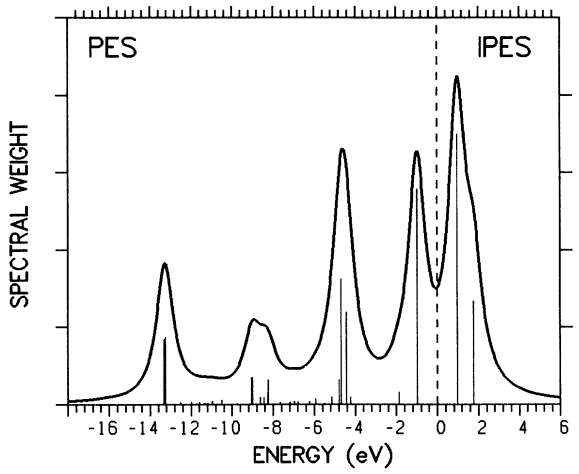


FIG. 1. Cu $3d_{x^2-y^2}$ electron-removal and -addition spectral weight for the $Cu_2O_7$ cluster, for the reduced basis set consisting of the $d_{x^2-y^2}$ and $p_\sigma$ orbitals only, and starting from the two-hole ground state, corresponding to the insulating materials. Positive-energy values correspond to electron-addition states and negative ones to electron-removal states. The solid line is a 1 eV full width at half maximum (FWHM) Lorentzian broadening of the discrete levels (vertical lines).

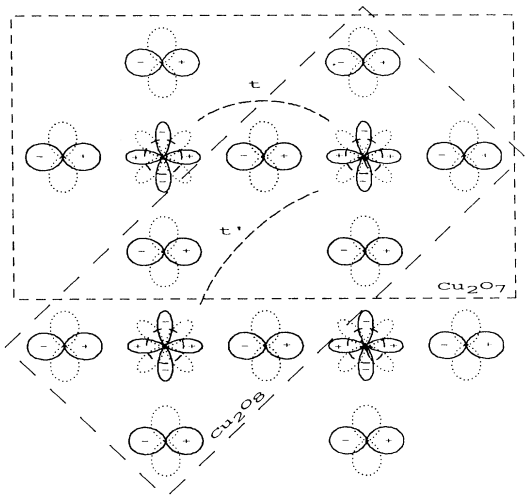


FIG. 2. $Cu_3O_7$ and $Cu_2O_8$ clusters.

$Cu_2O_7$-$Cu_2O_8$ calculation we report here, the maximum size of the matrices is about 2500, and the photoemission spectra consists of the order of 20 000 eigenvalues. Extending the size of the cluster to include four Cu atoms ($Cu_4O_8$ periodic) would increase this number to about $12\times10^6$ Slater determinants.

In this paper we will include the above considerations in calculations of spectral weights in PES and IPES, as well as core-level spectroscopies like x-ray absorption (XAS) or electron-energy-loss spectroscopy (EELS) and XPS for both the O 1*s* and Cu 2*p* core levels. We will concentrate especially on the dependence of the spectral shapes on doping.

## CALCULATIONS

The $Cu_2O_7$ and $Cu_2O_8$ clusters (see Fig. 2) have been introduced in previous work.[22] That paper was mainly concerned with the energy and character of the lowest-lying states. These states were compared with singlet-spin trial wave functions, and the parameters appearing in a *t-t'-J* model were estimated. Because of this introduction, we will only give a brief description of the ingredients of the calculation.

As mentioned above, the five Cu 3*d* and three O 2*p* orbitals are included. The one-electron part of the Hamiltonian is described in terms of a set of tight-binding parameters.[23] The various Cu-O transfer integrals can be expressed in terms of two parameters $pd\sigma$ and $pd\pi$, and the O-O matrix elements in terms of $pp\sigma$ and $pp\pi$. The two-electron part of the Hamiltonian contains several contributions. First, the atomic Coulomb and exchange interactions on copper are described by the three Racah parameters ($A,B,C$). The Racah $B$ and $C$ give rise to a spreading of the $d^8$ configurations over an energy range of about 7 eV. Second, the interactions on the oxygen site are described by two (Slater) integrals $F_0$ and $F_2$. Here $F_2$ is responsible for the atomic multiplet structure. All parameters are listed in Table I, taken from Ref. 22. The parameters were largely determined by means of fits of cluster and impurity calculations to photoemission data, as described elsewhere (see, for instance, Ref. 21). From Auger measurements on $Cu_2O$, the intersite Coulomb interaction $U_{pd}$ is estimated to be small (0–1 eV).[24] In the calculations its value is set to zero.

For PES and BIS we focus our attention mainly on Cu 3*d* emission or absorption of electrons, which is assumed to be described best because of the complete surrounding with neighboring oxygen atoms. For high photon energies the cross section of copper is about 30 times the cross section of oxygen. Therefore, the calculations are to be compared with XPS measurements. The same holds for the high-energy BIS experiment.

TABLE I. Parameter values. All energies in eV.

| | | | | |
|---|---|---|---|---|
| $\varepsilon_d$ | 0 | $A$ | 6.5 | $U_d=A+4B+3C=8.8$ |
| $\varepsilon_p$ | 3.5 | $B$ | 0.15 | $U_p=F_0+0.16F_2=6.0$ |
| $pd\sigma$ | 1.5 | $C$ | 0.58 | |
| $pd\pi$ | −0.7 | $F_0$ | 5 | $t_{pd}=\frac{1}{2}\sqrt{3}pd\sigma=1.3$ |
| $pp\sigma$ | −1.0 | $F_2$ | 6 | $t_{pp}=\frac{1}{2}(pp\pi-pp\sigma)=0.65$ |
| $pp\pi$ | 0.3 | $U_{pd}$ | 0 | |

The (angle-integrated) spectral distribution in the case of $d$ emission is calculated in the sudden approximation using the expression

$$I(\varepsilon_{e^-}) \propto \sum_F |\langle F,N+1|\hat{O}|\mathrm{GS},N\rangle|^2 \times \delta(E_{\mathrm{GS}}+\hbar\omega-E_F-\varepsilon_{e^-}) , \quad (1)$$

$$\hat{O} \propto \sum_{\Gamma,\sigma,\alpha} d^{\dagger}_{\Gamma,\sigma,\alpha} .$$

Here $N$ is the number of holes measured from the full band $d^{10}p^6$ system. $|\mathrm{GS},N\rangle$ is the $N$-hole ground state. $d_{\Gamma,\sigma,\alpha}$ is a hole-annihilation operator for a hole with symmetry $\Gamma$ and with spin $\sigma$. $\alpha$ labels one of the five $d$ orbitals ($x^2-y^2$, $3z^2-r^2$, $xy$, $xz$, and $yz$). Because the orbital determines for a large part the symmetry, the two labels $\alpha$ and $\Gamma$ are not independent. The $(N+1)$-hole state thus created is projected onto all the $(N+1)$-hole eigenstates $|F,N+1\rangle$. $\hbar\omega$ is the (constant) energy of the incoming photon, and $\varepsilon_{e^-}$ is the energy of the outgoing free electron, which is probed in the experiment. Equation (1) can be rewritten in terms of the one-hole Green's function

$$I(\varepsilon_{e^-}) \propto \pi^{-1}\mathrm{Im}[\langle \mathrm{GS},N|\hat{O}^{\dagger}\hat{G}(E_{\mathrm{GS}}+\hbar\omega-\varepsilon_{e^-}-i\delta) \times \hat{O}|\mathrm{GS},N\rangle] , \quad (2)$$

$$\hat{G}(z)=(z-\hat{H})^{-1} .$$

Similar expressions are used for IPES and core-level spectroscopies by using appropriate final states and replacing the operator $O$ appropriately.

To solve these expressions we use the following procedure. First the $N$-hole Hamiltonian matrix is written down. The ground state is then solved by means of a Lanczos-like method. The final-state Hamiltonian ($N+1$ holes in the case of photoemission) is rewritten in tridiagonal form, and the spectral Green's function is expressed in terms of a continued fraction.[25] The size of the matrices is reduced by exploiting the point-group symmetry of the clusters.

## DOPING DEPENDENCE OF PES AND IPES

In Fig. 3 we show the Cu $d$-electron-removal spectral weight for $N=0$, 1, and 2 holes in the ground state. The zero of energy for the one- and two-hole ground-state cases is the center of the band gap (halfway between the first electron-removal and first electron-addition states). Therefore, the gap can be obtained directly from the figure in these two cases. The two-hole ground state corresponds to the insulating undoped case, whereas the one-hole ground state corresponds to 50% electron doping.

The upper spectrum in Fig. 3 [Fig. 3(a)] describes emission from the full-band $d^{10}p^6$ system. Because of the absence of holes in the $d^{10}p^6$ state, the electron-removal spectrum is identical to that which one would obtain from an independent particle picture. The lower-energy states (0–2 eV) are of mainly $d$ character, and the states with mainly $p$ character lie in the region from 4 to 8 eV

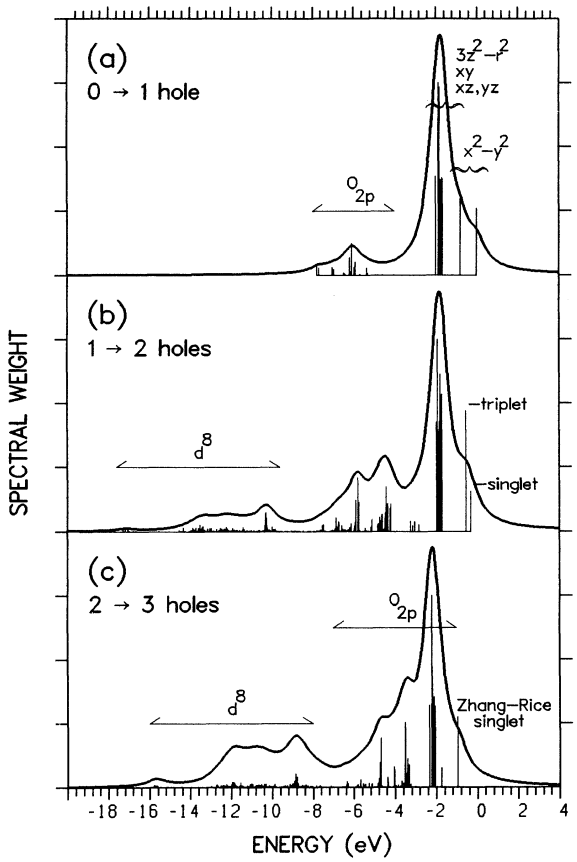


FIG. 3. Cu $3d$ spectral weights for the $Cu_2O_7$ cluster, for zero, one, and two holes in the ground state. (a) Emission from the full shell system. (b) Photoemission for the 50% electron-doped materials. (c) Spectral weight in the case of the undoped insulating materials. The solid line is a 1-eV FWHM Lorentzian broadening of the discrete levels (vertical lines).

binding energy. This spread of oxygen levels over about 4 eV is due to the intrinsic width of the oxygen band. The basic features of this spectrum are close to those found in the PES spectrum of $Cu_2O$.[26] In the $d$ part of the spectrum, we see the ligand field split Cu $3d^9$ states as marked. These correspond closely to the ground-state or optical-absorption (one-hole) calculations of a $CuO_4$ cluster,[12] in which we found a lowest-energy $d_{x^2-y^2}$ ($b_1$) state and the states of $a_1$, $e$, and $b_2$ symmetry clustered at 1.5 eV above this ground state. Upon making the cluster larger, one expects to see some "banding" of the $d_{x^2-y^2}$ state because of its strong covalent mixing as compared to the $3z^2-r^2$, $xy$, $xz$, and $yz$ states. This is why the $d_{x^2-y^2}$ state is split into a bonding and antibonding state with separation of 0.8 eV in the $Cu_2O_7$ cluster.

Upon adding one hole to the initial state, which would correspond to a 50% electron-doped CuO system, the final state in photoemission involves two holes. The lowest-energy part [see Fig. 3(b)] again shows the splitting between the $x^2-y^2$ and the $3z^2-r^2$, $xy$, $xz$, and $yz$ orbitals. In a pure one-electron picture, we would still

expect to see the bonding-antibonding splitting since an electron can still be removed from the antibonding or the bonding orbital with now an intensity ratio of 1:2. Because of the large $U$, however, this picture changes dramatically in the low-energy-scale part. What we see are indeed two peaks with an intensity ratio of 1:3, but these now correspond to the singlet and triplet states of two holes in the cluster. Comparison with the previous spectrum shows nicely how we must go from a one-electron molecular-orbital picture if we have only one hole, and to a Heitler-London picture if we have two holes with $U$ large. The small splitting between these two configurations is just the superexchange interaction $J$.[22,27-29] The intensity ratio between these two peaks is mainly determined by the difference in degeneracy of the triplet and singlet states. In addition, we see the appearance of a low-intensity, high-energy feature (9–17 eV) in Fig. 3(b), corresponding to Cu $d^8$-like final states which now can be reached. This $d^8$-like part which involves $U$ corresponds to the high-polarity states in the Heitler-London picture. The BIS spectrum for this case is trivial. It consists of one peak at zero energy, corresponding to the filling of the antibonding $b_1$ state of Fig. 3(a).

The situation changes as we go to the PES spectrum of the two-hole system (bottom curve). Now, because $U$ is large, the two holes are correlated with one hole at each Cu site. By removing another $d$ electron, we no longer can easily avoid $U$. The consequence is a large $d^8$ amplitude in the region 10–14 eV. Even more important is that the low-energy-scale part can no longer be obtained from the curves in Figs. 3(a) or 3(b) in a simple way.

It is interesting to see what would happen if the Cu-O hybridization were zero. Then the two-hole case would imply one hole on each Copper site. From the correlation point of view, this corresponds to a "half-filled" band case. Because of the large Hubbard $U$, the $d$-spectral weight will consist of only high-energy levels, corresponding to the part above 8 eV n Fig. 3(c) (or Fig. 4). That the spectra, as seen in photoemission experiments, show their largest signal in the region below 8 eV is a consequence of the largely covalent nature of these materials. The two-hole ground state from which the extra electron is removed to obtain Fig. 3(c) contains 0.66 $d$ holes and in total 0.34 O $2p$ holes per Cu site. These 0.34 O $2p$ holes, however, are distributed over four oxygens so that each oxygen has only 8% holes transferred from one neighboring Cu. The lowest-energy electron-removal state contains 0.79 $d$ holes and 0.71 O $2p$ holes per Cu site, showing that it is primarily (for about 75%) an O $2p$ electron which is removed, but also showing that all these states are strongly hybridized.

In Fig. 4 we show the combined electron-removal and -addition spectrum from the two-hole ground state, which should be compared with the combined XPS and BIS measurements for the undoped system. The zero energy corresponds again to the center of the insulating band gap. The band gap is equal to the energy difference between the first electron-addition and -removal states, or

$$E_{\text{gap}} = E_{\text{GS}}(3 \text{ holes}) + E_{\text{GS}}(1 \text{ hole}) - 2E_{\text{GS}}(2 \text{ holes}) , \quad (3)$$

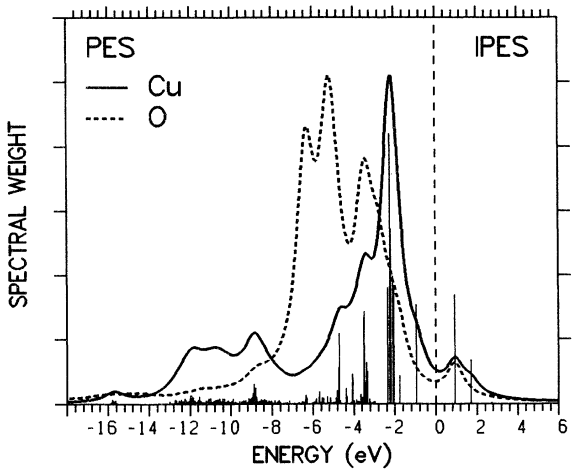


FIG. 4. Cu $3d$ (solid curve and vertical lines) and central oxygen O $2p$ (dashed curve) electron-removal and -addition spectral weight for the $Cu_2O_7$ cluster, starting from the two-hole ground state. Positive-energy values correspond to electron-addition states and negative ones to electron-removal states. The solid and dashed lines are 1-eV FWHM Lorentzian broadenings of the discrete levels.

which is $\sim 1.9$ eV for the $Cu_2O_7$ cluster. As already mentioned, the part of the spectrum roughly above 8 eV is mainly due to the $d^8$ multiplets. The small peak at 16 eV is a high-energy $d^8$ singlet ($^1S$ in spherical symmetry). The other singlet configurations have most of their weight at high energy (above 11 eV) and the triplets at lower energies (8–12 eV). In a resonant photoemission experiment, the strongest enhancement is to be expected for the high-orbital-momentum $^1G$ (in spherical symmetry) $d^8$ multiplet, which is concentrated around 12 eV.[12,14,30]

In the lower-energy part of the spectrum, there is a concentration of levels around 2–2.5 eV with a large spectral weight. These are largely due to weakly dispersive $z$-oriented levels, like the $d_{xz}$, $d_{yz}$, and $p_z$ orbitals. The state at 1 eV binding energy is well described by a bonding combination of (Zhang-Rice[31]) singlet-spin trial wave functions.[22] The antibonding counterpart lies $\sim 0.8$ eV higher in energy and is separated by 0.3 eV from the "continuum" of states around 2 eV. Such splittings as between the bonding and antibonding states described above have been used in several studies[27,32,33] to arrive at a value for $t$ in a $t$-$J$ or $t$-$t'$-$J$ model for the hole-doped case, which describes the hopping of the Zhang-Rice singlet to a nearest-neighbor Cu atom. From this splitting we determined the value of $t$ to be $\simeq 0.4$ eV.[22]

If the photon energy is lowered, the relative cross section of the oxygen increases. In general, the PES spectrum will contain both Cu $3d$ and O $2p$ spectral weights. The dotted line in Fig. 4 shows the emission and absorption spectrum of electrons from the central oxygen site in the $Cu_2O_7$ cluster. Comparing this with the full line in Fig. 4, we would expect an increase of spectral intensity

in the region 4–6.5 eV in going from XPS to ultraviolet photoemission spectroscopy (UPS). In this case one should be cautious about simply adding the two curves, because this will give only the incoherent sum, while coherence effects between emission from Cu and O will change the intensities significantly.[34] The oxygen bandwidth is seen to be about 5 eV. Contrary to emission from copper, the main features of the $p$-spectral weight do not change much if one compares the $0\rightarrow 1$, $1\rightarrow 2$, and $2\rightarrow 3$ hole emission processes, in spite of the fact that $U_{pp}$ is quite large. This is explained by the low oxygen hole occupation number per site in all three cases. Note that the lowest-energy state is not reached by the emission from the central oxygen. The reason for this is that the added hole has to be symmetric around the central oxygen in order to connect the ground state with this first electron-removal state, while a $p$ orbital is antisymmetric. This lowest-energy state none the less has overall 1.6 times as much O $p$- than Cu $d$-spectral weight,[12] arising from the other oxygens.

Figure 4 also shows the BIS spectrum from the two-hole ground state. The main peak can be labeled $d^{10}d^9$ (one Cu is $d^{10}$ and the other $d^9$) as one ends up in a locally filled shell system. This peak is split into a bonding and antibonding part with a splitting of about 0.8 eV, as in the PES spectrum from the zero-hole ground state [Fig. 3(a)]. This can be compared with the BIS spectrum of CuO or the high-$T_c$ compounds.[35–37]

More interesting is the BIS spectrum starting from the three-hole ground state, corresponding to the 50% hole-doped case (Fig. 5). The signal now consists of two parts: a $d^9d^9$ part around 0 eV energy and a $d^{10}d^9\underline{L}$ part at 2–3 eV. Note that, although we label the state $d^9d^9$, this is a strongly hybridized state and involves a large $d^{10}\underline{L}d^9$ component. Here again it is interesting to compare this spectrum with the spectrum one would get in the case of zero or small hybridization. Because of the large value for $U_{dd}$, the initial state has hardly any $d^8$ character, but is then mainly of $d^9d^9\underline{L}$ character. Thus we expect a very-low-intensity $d^9d^9$ peak when one adds an electron to the Cu $3d$ shell, as in the high-energy BIS experiment. However in Fig. 5 this $d^9d^9$ peak actually dominates, which is a result of hybridization. This strong shift of spectral weight from the upper Hubbard band to the Fermi level with hole doping could play a very important role in the high-$T_c$ materials and is a general result of constructive interference of the various channels for the lowest-energy states in hybridized systems. The states around 6 eV in Fig. 5 correspond to $d^{10}\underline{L}d^{10}\underline{L}$-like states.

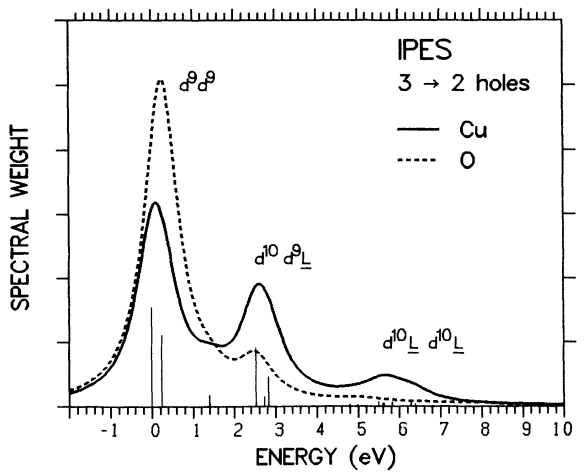


FIG. 5. Cu $3d$ (solid curve and vertical lines) and central oxygen O $2p$ (dashed curve) electron-addition spectral weight for the $Cu_2O_7$ cluster, starting from the three-hole ground state. FWHM = 1 eV.

Besides the large features mentioned above, we also find a small peak at 1.4 eV. This peak does not exist in case we use only the reduced basis consisting of $d_{x^2-y^2}$ and $p_\sigma$ orbitals. The three-hold ground state has a $d_{3z^2-r^2}$ occupation of $\sim 0.013$ per Cu site, and the peak at 1.4 eV can be interpreted as a $d_{x^2-y^2}\rightarrow d_{3z^2-r^2}$ excitation. However, although this peak is due to the $d_{3z^2-r^2}$ orbitals, it is mainly reached by means of $d_{x^2-y^2}$ electron addition. Without this small peak, the spectrum using the full basis and the spectrum for the reduced basis are almost identical. This suggests that a reasonable description of the inverse photoemission (up to a few eV) can be obtained using only the restricted basis set.[18] Note that the mixing of $d_{x^2-y^2}$ and $d_{3z^2-r^2}$ is symmetry forbidden in the $CuO_4$ cluster, but in the two copper clusters or in the translational symmetric material, this mixing is allowed at k values far from $\Gamma$, like $(\pi,0)$ in the two-dimensional (2D) $CuO_2$ plane.

Also shown in Fig. 5 is the O $2p$ electron-addition spectrum, again for the central oxygen atom in the $Cu_2O_7$ cluster. Here we see that for the hole-doped system the threshold peak is very strong indeed, indicating its predominant ligand hole character.

## CORE-LEVEL SPECTROSCOPIES: Cu $2p$

It is well known that the core Cu $2p$ line shape is strongly dependent on the number of $d$ holes in the ground state.[38] This dependence is clearly evidenced by the very large satellite in Cu $2p$ XPS of CuO and its absence in $Cu_2O$.[35,39] The large satellite for CuO is caused by the fact that the core-hole potential in the final state prefers the strongly screened $d^{10}$ local configuration. Thus the energy-level diagram is the reverse of that for the ground state; i.e., the final-state $d^{10}\underline{L}\underline{c}$ configuration is lower in energy than $d^9\underline{c}$. The intensity of the satellite is determined by the hybridization (and the related $d^9$ occupation) in both the ground and final states. As discussed in detail elsewhere,[38] the satellite structure is very weak in XAS or EELS at the Cu $2p$ edge because here the photoexcited electron can serve as the screening electron, and a charge redistribution (as must occur in XPS) is no longer required.

For both the XAS and XPS core-level spectra, one needs to know the core-hole binding energy. The absolute values of the energies for XPS are related to those of XAS by means of this energy. One, however, has to be careful because the different spectra all involve different numbers of holes in the valence band. To obtain the en-

ergy offset for the calculated core-level spectra, we used the following procedure. First, we define the chemical potential for different numbers of holes (without the core hole). For the insulating two-hole case, the chemical potential is taken to lie in the middle of the insulating band gap. The same thing is done for the one-hole case. In the latter case the gap is small [see Fig. 3(b)] and is due to the finite size of the $Cu_2O_7$ cluster. As the hole-doped case is also expected to have a small gap (if any), the three-hole chemical potential is taken at the position of the first electron-removal state in Fig. 4. Then all one-particle energies (including now the core-hole binding energy) are shifted in such a way that this chemical potential is equal to zero. The energy shifts required are 1.83, 0.60, and $-0.34$ eV for the one-, two-, and three-hole ground states, respectively. For a certain value of the core-hole–valence-hole Coulomb interaction $Q$, the core-hole binding energy is determined by shifting the two-hole XPS spectrum until the energy value of the main peak coincides with the measured binding energy in the XPS experiment for the undoped $La_2CuO_4$ compound.[40] This determines all the other energies.

Since the Cu $2p$ spectra have been discussed in detail elsewhere, we show them here just for comparison. The calculations are restricted to a $CuO_4$ cluster for simplicity. The spectra for, say, a Cu $2p_{3/2}$ core hole are shown in Fig. 6(b) for a Cu $2p$–Cu $3d$ interaction $Q=9.3$ eV. The $2p$-$3d$ repulsion $Q$, which contributes to the energy difference between the $d^9$ and and $d^{10}\underline{L}$ peaks in Fig. 10(b), is obtained by comparing the $d^9$ peak position with experimental data. In general the on-site core-hole–valence-hole Coulomb matrix element is somewhat larger than the valence-hole–valence-hole repulsion. The value of $Q$ found here is 38% larger than the average $3d$-$3d$ interaction (Table I). In the calculation we have

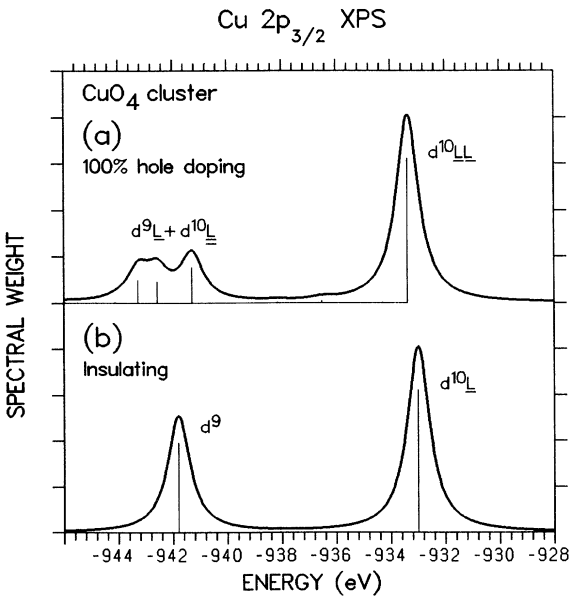


FIG. 6. Cu $2p$ core-level x-ray photoemission spectrum from the $CuO_4$ cluster, for the two-hole (top curve) and one-hole (bottom curve) ground states. The core-hole potential $Q$ is 9.3 eV. FWHM=1 eV.

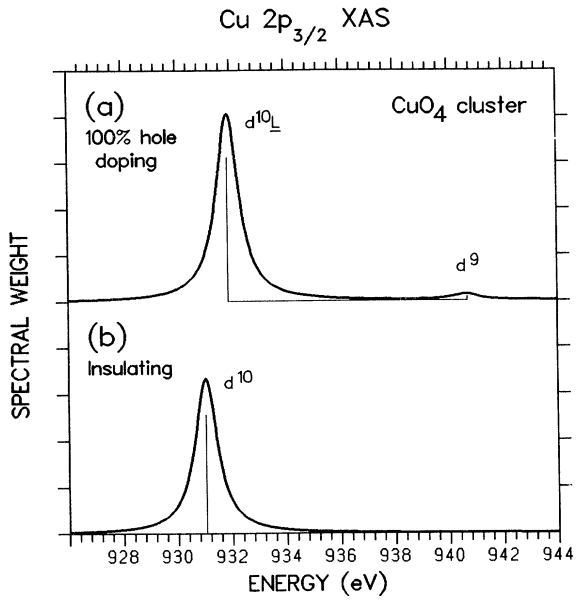


FIG. 7. Cu $2p$ core-level x-ray absorption spectrum from the $CuO_4$ cluster, for the two-hole (top curve) and one-hole (bottom curve) ground states. $Q=9.3$ eV. FWHM=1 eV.

neglected the multiplet structure in the $d^9$ peak which is so evident in the experimental spectra and which has been discussed in detail by van der Laan *et al.*[38] and more recently for the high $T_c$'s by Okada and Kotani.[15]

For the small $CuO_4$ cluster, neglecting these multiplets, the ground and final states are both described by $2\times2$ matrix. For the ground-state problem, the configurations are $d^9_{x^2-y^2}$ and $d^{10}\underline{L}_{x^2-y^2}$ (hole on oxygen of $x^2-y^2$ symmetry), and in the final state these are $\underline{c}d^9_{x^2-y^2}$ and $\underline{c}d^{10}\underline{L}_{x^2-y^2}$. The point of interest here is the intensity of the satellite for the one-hole ground state, which is in good agreement with the core-level spectra of CuO.

In the case of two holes in the $CuO_4$ cluster [Fig. 6(a)], which would correspond to 100% hole doping, the relative weights between the main peak and satellite is comparable with what was found in the one-hole case [Fig. 6(b)]. This can be understood by noting that the holes added by doping charge-transfer insulators only increase the oxygen or ligand hole count significantly. The $d^9\underline{L}$ peak in the spectrum is split into smaller subpeaks because for $U_p\sim6$ eV the $\underline{c}d^9\underline{L}$ state is almost degenerate with a $\underline{c}d^{10}\underline{L}\underline{L}$ state with two holes on the same oxygen site, marked as $d^{10}\underline{L}$ in the figure. It will, however, not be easy to detect this splitting experimentally because of the even-larger multiplet splitting of this $\underline{c}d^9\underline{L}$ peak.

In the Cu $2p$ XAS experiment, the core electron stays at the Cu atom and therefore takes care of the screening of the core potential. Thus the satellite structure will be small. This effect is clearly seen in Figs. 7(a) and 7(b) for the two- and one-hole ground states, respectively.

## CORE-LEVEL SPECTROSCOPIES: O $1s$

Since the O $1s$-$2p$ Coulomb interaction will probably be large (certainly larger than $U_{pp}$), we might also expect

a rich satellite structure in the O 1$s$ XPS spectra. This, however, turns out not to be the case as we will now demonstrate.[41]

In $O_{1s}$ core-level XPS, a 1$s$ electron is ionized. The energy of the outgoing electron will strongly depend on the number of holes present in the 2$p$ shell of this specific oxygen site. In the sudden approximation the spectrum essentially consists of a projection of the valence-band ground state without a core hole on the eigenstates in the presence of the core-hole potential. The repulsion between the core hole and 2$p$ hole is treated again as a local potential on the core-hole site. Here the core-hole–2$p$-hole exchange interaction is neglected. This exchange is only of importance for the high-lying energy states where the oxygen with the core hole has five instead of six electrons in its 2$p$ shell.

In Fig. 8 we show the XPS spectrum calculated for one, two, and three holes in the $Cu_2O_7$ cluster, with the core hole located at the central oxygen site and for a core-hole–2$p$-hole interaction $Q_{1s\text{-}2p}=6$ eV, which is about 30% larger than the average 2$p$-2$p$ repulsion (Table I). The spectra all mainly consist of one large threshold peak containing 95%, 90%, and 85% of the total spectral weight for the one-, two, and three-hole cases, respectively. The weight of this peak is equivalent to the overlap squared between the ground states with and without the core hole present. Besides this peak there are several

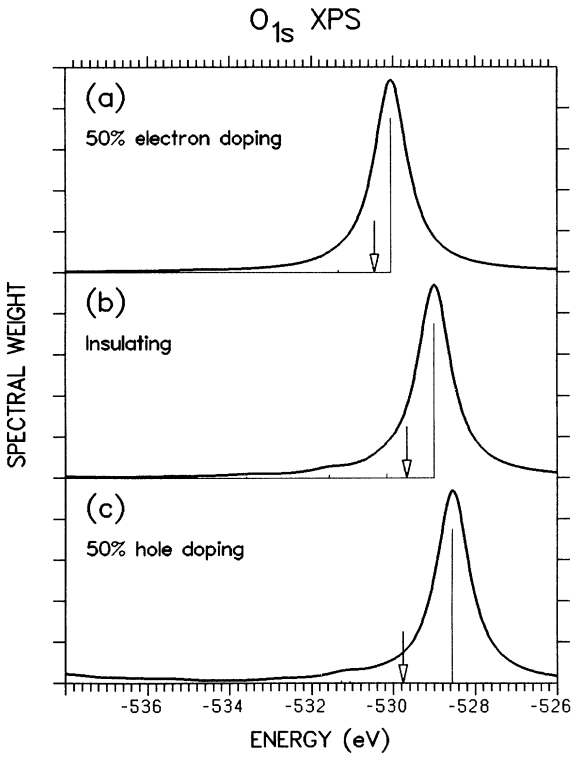


FIG. 8. $O_{1s}$ core-level x-ray photoemission spectrum with the core hole located at the oxygen site of the $Cu_2O_7$ cluster, for the one-hole (top curve), two-hole (middle), and three-hole (bottom curve) ground states. The core-hole potential is taken to be 6 eV. The arrows indicate the frozen ground-state Koopman's-theorem value for the core-hole binding energy. FWHM = 1 eV.

very-low-intensity states at higher energies, which will not be easy to detect in the actual XPS experiment. That these satellites are so low in intensity is a result of a relatively low density of O 2$p$ holes in the system. This "lack" of satellite structure is in agreement with the experimental $O_{1s}$ XPS spectra[38] for clean surfaces. In the literature one finds a multitude of $O_{1s}$ XPS spectra with multicomponent structures,[39] most of which we believe are a result of surface contaminations.

The arrows in Fig. 8 (and Fig. 9) indicate the Koopman's-theorem value for the binding energy of the core hole. This is calculated by freezing the ground-state charge distribution and then calculating the total energy in the presence of the core hole, and is equivalent to the weighted average energy over the main peak plus satellites. It is the Koopman's-theorem value of the binding energy which shows the shift with doping expected because of the 1$s$-2$p$ interaction. The shift of the main line is due mainly to the shift in the chemical potential. In other words, if we had used the vacuum level as a reference, the main line would hardly have shifted. The increasing energy difference between the Koopman's-theorem value and the position of the threshold line in Fig. 8 can be compared to $Q_{1s\text{-}2p}\times n_{2p}$, where $n_{2p}$ is the number of 2$p$ holes on the central oxygen. These occupations are 0.14, 0.21, and 0.37 for the one-, two-, and three-hole ground-state wave functions, respectively. Small differences from this are due to changing hybridization effects. This result shows very clearly that there is no simple relationship between the binding energy of the threshold peak and the effective charge, but that there is such a relationship if one considers instead the weighted average peak position. This has been a misconception in numerous papers on binding-energy shifts in XPS.

In Fig. 9 we investigate the influence of changing the core-hole–valence-hole repulsion $Q$ for the three-hole or 50% hole-doping case. For $Q=0$ [Fig. 9(a)] the spectrum consists of only one peak. In this case the charge distribution in the valence band is not influenced by the core hole, and there will thus be no satellite structure. As already mentioned, the 1$s$-2$p$ repulsion will manifest itself only in states with holes on the oxygen, i.e., in the high-energy low-intensity satellite structure. In Fig. 9 there are indeed some small changes in the part above 530 eV, comparing $Q=4$ with $Q=8$. Note that these small satellites stretch to far below $-537$ eV.

The effects of the strong hybridization between the Cu 3$d$ and O 2$p$ levels do not only show up in the photoemission and inverse photoemission spectra, but it also strongly influences the shape of the $O_{1s}$ XAS spectra. In the XAS experiment an oxygen 1$s$ core electron is promoted to the 2$p$ level of the same atom. The spectral distribution is again given by an expression like Eq. (1), but now the operator creates a 2$p$ electron on the central oxygen site in the $Cu_2O_7$ cluster, and the [$(N-1)$-hole] final states are calculated with the core hole present.

In Fig. 10 we show the XAS spectra starting from the two-hole [Fig. 10(b)] and three-hole [Fig. 10(a)] ground states. Figure 10(a), which is the spectrum starting from a three-hole (50% hole-doping) ground state, consists of two main parts. The large peak at 528 eV is reached by

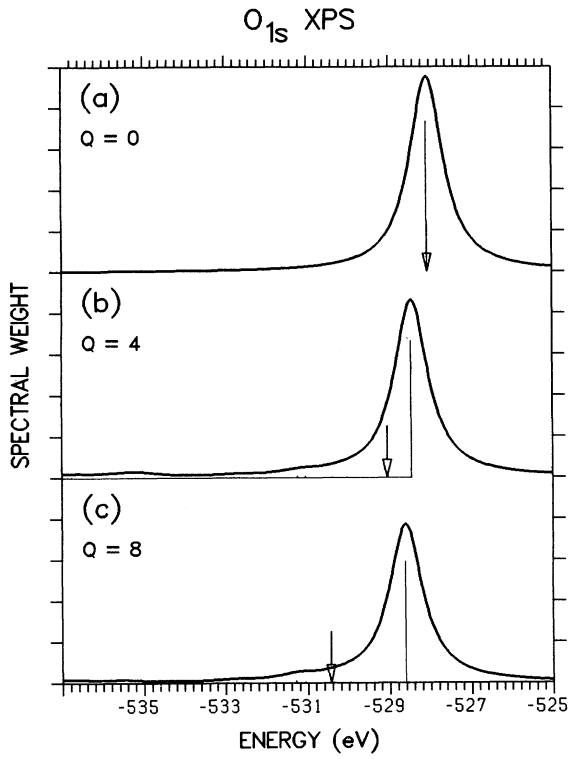


FIG. 9. $O_{1s}$ core-level x-ray photoemission spectrum with the core hole located at the central oxygen site of the $Cu_2O_7$ cluster, for different values of the $1s$-$2p$ Coulomb matrix element $Q$, calculated for the three-hole or 50% hole-doping case. The arrows indicate the Koopman's-theorem value for the core-hole binding energy. FWHM = 1 eV.

promoting the core electron to the top of the ligand band and can be labeled $d^9d^9$. A second, smaller peak at 530–531 eV corresponds to the upper Hubbard band ($d^{10}d^9\underline{L}$). The distance between the ligand and upper Hubbard peaks is somewhat larger than the band-gap value obtained from Eq. (3), because of the hybridization between these two bands. The XAS spectrum for the insulating case [Fig. 10(b)] consists of essentially one peak, corresponding to the upper Hubbard band ($d^{10}d^9$).

A prominent feature of Fig. 10 is the strong decrease in intensity of the $d^{10}$ or upper Hubbard band state in going from the two-hole [Fig. 10(a)] to the three-hole [Fig. 10(b)] ground-state case. This effect has clearly been observed in the XAS spectra of Li-doped NiO,[42] and is a direct result of the strong hybridization.

Because of the very low double occupation ($p^4$) on the central oxygen site, the final state in the XAS process is almost purely $p^6$. As the core-hole potential is only present in the final state, the spectrum is expected to be quite insensitive to the actual value of the core-hole–$2p$-hole repulsion. In Fig. 11 we show the three- to two-hole XAS spectra for various values of this repulsion $Q$ [see also Fig. 10(a)]. As can be seen, there is hardly any change in the shape of the spectra in going from $Q = 0$ (corresponding to IPES on the central oxygen site) to $Q = 8$ eV.

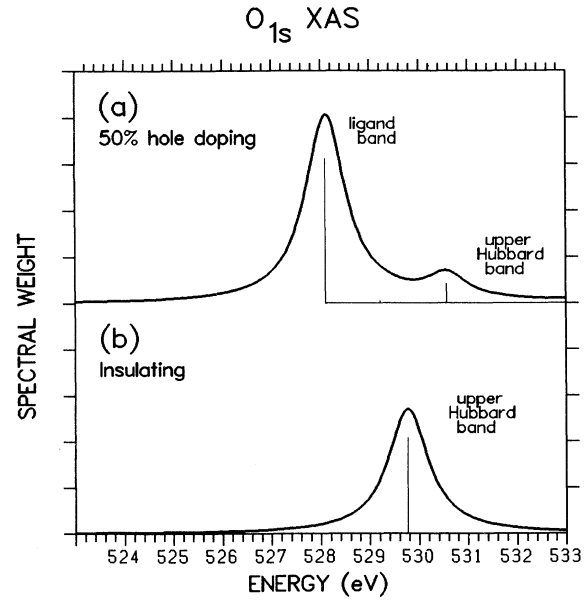


FIG. 10. $O_{1s}$ core-level x-ray absorption spectrum with the core hole located at the central oxygen site of the $Cu_2O_7$ cluster, for the three-hole (top curve) and two-hole (bottom curve) ground states. The core-hole potential is taken to be 6 eV. FWHM = 1 eV.

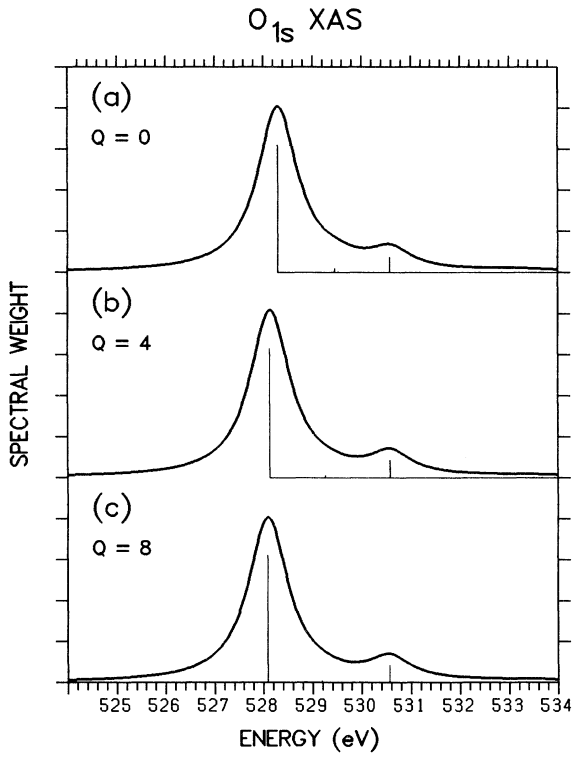


FIG. 11. $O_{1s}$ core-level x-ray absorption spectrum with the core hole located at the central oxygen site of the $Cu_2O_7$ cluster, for different values of the $1s$-$2p$ Coulomb matrix element $Q$, calculated for the three-hole or 50% hope-doping case. FWHM = 1 eV.

An important conclusion in comparing the XPS to XAS threshold lines is that these all come at nearly the same binding energies, independent of the choice of $Q_{1s\text{-}2p}$. This is so even if this interaction is large enough to pull out an excitonic state. A comparison of XPS and XAS energies therefore does not in this case provide information about whether or not core-hole excitons are involved. This again is a result of the low $O_{2p}$-hole concentration.

## COMPARISON OF SPECTRA OBTAINED FOR VARIOUS CLUSTERS OR AN IMPURITY APPROACH

To get a feeling for the sensitivity of the spectra on cluster size and the way the oxygen levels are treated, we compare the spectrum of Fig. 4 with several other calculations using the same set of parameters (given in Table I). In Fig. 12(c) the XPS spectrum of a $Cu_2O_8$ cluster is shown. This cluster, shown in Fig. 2, consists of two next-nearest-neighbor Cu atoms and their four surrounding oxygens. The overall shape of the photoemission spectrum is very similar to the one shown in Fig. 4 [or Fig. 12(d), which shows again the XPS spectrum for the $Cu_2O_7$ cluster for comparison]. The $d^8$ part has changed only little in shape, but has become a little broader. Most of the changes occur in the $d^9\underline{L}$ part below 8 eV, as is to be expected because mainly the oxygen levels will be different. The bonding and antibonding singlet-spin combinations are closer together than in the $Cu_2O_7$ case, resulting in $t' < t$, as shown previously,[22] and are more clearly separated from the levels around 2.5 eV. The energy gap is $\sim 1.95$ eV.

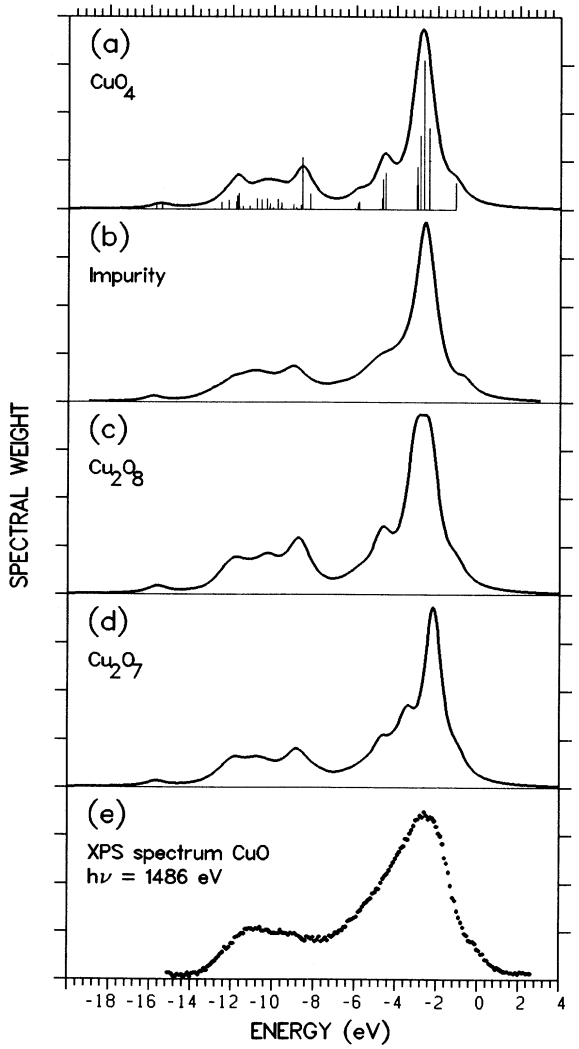


FIG. 12. Photoemission spectra for the undoped materials, calculated by means of (a) a $CuO_4$ cluster, (b) an impurity calculation, (c) a $Cu_2O_8$ cluster, and (d) the $Cu_2O_7$ cluster. FWHM=1 eV. The bottom curve ($E$) is the experimental XPS spectrum for CuO, taken from Ref. 35.

In Fig. 12(a) the results for a $CuO_4$ cluster are shown.[12] The first electron-removal "local singlet" state now consists of only one level and is clearly separated from the levels around 2.5 eV. The $d^8$ part of the spectrum is broader than in Fig. 12(d); thus increasing the size of the cluster seems to decrease this width. The overall shape is, however, very similar to that of Fig. 12(d). The band gap is 2.2 eV, 0.3 eV larger than for $Cu_2O_7$. Hybertsen *et al.*[32] have studied a sequence of clusters, starting from $CuO_4$ up to $Cu_5O_{16}$, using the reduced basis set. They also find a decrease of the band gap with the size of the cluster. Their gap for $CuO_4$ is about 0.6 eV larger than for $Cu_2O_7$. Thus we find a less pronounced effect here.

Figure 12(e) shows the measured XPS spectrum for CuO, taken from Ref. 35. As discussed in a previous paper,[12] CuO resembles the high-$T_c$ materials in quite a few aspects, like, for instance, the value of the superexchange interaction, the shape of the Cu $2p$ core-level XPS spectrum, the local surrounding of the Cu atom, etc. The overall shape and intensities of the valence-band XPS spectrum for CuO are taken as being characteristic of those measured for the high-$T_c$ compounds.

Finally, the results of Fig. 4 [Fig. 12(d)] are compared with an impurity calculation.[13] Here a single Cu "impurity" atom is placed in the square lattice of in-plane oxygens. Correlation effects are treated explicitly on the Cu site only. Starting from full bands, the antiferromagnetic compounds (one hole per Cu) correspond to the one-hole solution. The one-electron part of the Hamiltonian is given by

$$H_0 = \sum_{\alpha,\sigma} \varepsilon_\alpha d^\dagger_{\alpha,\sigma} d_{\alpha,\sigma} + \sum_{\mathbf{k},\beta,\sigma} \varepsilon_\beta(\mathbf{k}) C^\dagger_{\beta,\mathbf{k},\sigma} C_{\beta,\mathbf{k},\sigma} + \sum_{\alpha,\mathbf{k},\beta,\sigma} [V_{\alpha\beta}(\mathbf{k}) C^\dagger_{\beta,\mathbf{k},\sigma} d_{\alpha,\sigma} + \text{H.c.}] \,. \quad (4)$$

Here the first term counts the number of holes on Cu ($\alpha \in 1, \ldots, 5$) with spin $\sigma$. The second term counts the number of oxygen holes in the Bloch state with momentum $\mathbf{k}$. $\beta$ labels the three different oxygen $2p$ orbitals. The last term describes the $\mathbf{k}$-dependent coupling of the Bloch states with the Cu site. The one-hole Green's function can be written down in terms of the double integral over $\mathbf{k}$, which is evaluated numerically:

$$\langle d,\alpha|\hat{G}|d,\alpha\rangle = \left[ z - \varepsilon_\alpha - \frac{1}{(2\pi)^2} \int d\mathbf{k} \sum_\beta \frac{V_{\alpha\beta}(\mathbf{k})^2}{z - \varepsilon_\beta(\mathbf{k})} \right]^{-1} , \quad (5)$$

and, for example,

$$\varepsilon_x(\mathbf{k}) = 2pp\sigma \cos k_x + 2pp\pi \cos k_y \ ,$$
$$V_{x^2-y^2,x}(\mathbf{k}) = 4i\sqrt{6}\, p\, d\sigma \cos(\tfrac{1}{2}k_x)\sin(\tfrac{1}{2}k_y) \ . \quad (6)$$

The photoemission spectrum, equivalent to adding a second hole, requires the solution of the two-hole problem. Now the two-electron (or two-hole) part of the Hamiltonian has to be included. It consists of all the different Coulomb multiplet interactions of two holes in the $3d$ shell of the Cu, written in terms of the Racah $A$, $B$, and $C$ parameters. The exact solution of this two-hole problem can be expressed in terms of the one-hole Green's functions given by Eq. (5). For details the reader is referred to Refs. 13 and 34. The results of the calculations are shown in Fig. 12(b). Again, the result compares favorably with experiment. At the lower side of the $d^9\underline{L}$ band (between 2 and 8 eV binding energy), a discrete singlet bound state is pushed out of the band. This state has the symmetry and spin of a low-spin $Cu^{3+}$ ($d^8$) state, but with one of the holes primarily on the oxygen. This state looks like a Haldane-Anderson[43] multiply charged impurity state in semiconductors. The gap is somewhat smaller than for the clusters (namely, 1.65 eV), which is largely due to the neglect of oxygen-oxygen correlations. Inclusion of these correlations will increase the gap by about 0.2 eV.

In conclusion, we have presented calculations of the photoemission and inverse photoemission spectra and O $1s$ core-level spectroscopies for high-energy incoming photons for two clusters containing two Cu atoms, namely, $Cu_2O_7$ and $Cu_2O_8$. The photoemission results were compared with earlier work ($CuO_4$ and impurity calculations) and were found to be different only in the smaller details, within an energy resolution of about 0.5 eV. It was found that the calculated oxygen $1s$ core-level XPS has a weak and very smeared out satellite structure, in contrast to the Cu $2p$ XPS spectrum. The BIS and O $1s$ core-level XAS spectra for the hole-doped case showed a strong decrease of intensity of the upper Hubbard band as compared to the insulating case, due to the transfer of spectral weight to the oxygen band. Furthermore, attention was paid to the doping dependence of the spectra.

## ACKNOWLEDGMENTS

We would like to thank L. F. Feiner for valuable discussions and remarks, and a careful reading of the manuscript. This investigation was supported by the Netherlands Foundation for Chemical Research (SON) and the Netherlands Foundation for Fundamental Research on Matter (FOM) with financial support from the Netherlands Organization for the advancement of Pure Research (NWO).

[1] *High Temperature Superconductivity,* Proceedings of the Los Alamos Symposium, Los Alamos, New Mexico, 1989, edited by K. Bedell, D. Coffey, D. E. Meltzer, D. Pines, and J. R. Schrieffer (Addison-Wesley, Reading, MA, 1990).
[2] C. A. Balseiro, M. Avignon, A. G. Rojo, and B. Alascio, Phys. Rev. Lett. **62**, 2624 (1989).
[3] W. A. Pickett, Rev. Mod. Phys. **61**, 433 (1989).
[4] A. K. McMahan, R. M. Martin, and S. Satpathy, Phys. Rev. B **38**, 6650 (1988).
[5] M. S. Hybertsen, M. Schlüter, and N. E. Christensen, Phys. Rev. B **39**, 9028 (1989).
[6] L. F. Mattheiss and D. R. Hamann, Phys. Rev. B **40**, 2217 (1989).
[7] M. J. De Weert, D. A. Papaconstantopoulos, and W. E. Pickett, Phys. Rev. B **39**, 4235 (1989).
[8] S. Tajima, S. Tanaka, T. Ido, and S. Uchida (unpublished).
[9] Z. Shen *et al.,* Phys. Rev. B **36**, 8414 (1987).
[10] A. Fujimori, Phys. Rev. B **39**, 793 (1989).
[11] F. Mila, Phys. Rev. B **38**, 11 358 (1988).
[12] H. Eskes, L. H. Tjeng, and G. A. Sawatzky, Phys. Rev. B **41**, 288 (1990).
[13] H. Eskes and G. A. Sawatzky, Phys. Rev. Lett. **61**, 1415 (1988).
[14] O. Gunnarsson, J. W. Allen, O. Jepsen, T. Fujiwara, O. K. Anderson, C. G. Olsen, M. B. Maple, J. S. Kang, L. Z. Liu, J. H. Park, R. O. Anderson, W. P. Ellis, R. Liu, J. T. Markert, Y. Dalichaouch, Z. X. Shen, P. A. P. Lindberg, B. O. Wells, D. S. Dessau, A. Borg, I. Lindau, and W. E. Spicer, Phys. Rev. B **41**, 4811 (1990).
[15] K. Okada and A. Kotani, J. Phys. Soc. Jpn. **58**, 1095 (1989); **58**, 2578 (1989).
[16] Y. Kuramoto and H. J. Schmidt, in *Strong Correlation and Superconductivity,* Vol. 89 of *Springer Series in Solid-State Sciences,* edited by H. Fukuyama, S. Maekawa, and A. P. Malozemoff (Springer-Verlag, Berlin, 1989), p. 88.
[17] P. Horsch, W. H. Stephan, K. v. Szczepanski, M. Ziegler, and W. von der Linden, Physica C **162-164**, 783 (1989).
[18] P. C. Pattnaik and D. M. Newns, Phys. Rev. B **41**, 880 (1990).
[19] C. A. R. Sá de Melo and S. Doniach, Phys. Rev. B **41**, 6633 (1990).
[20] E. Antonides, E. C. Janse, and G. A. Sawatzky, Phys. Rev. B **15**, 1669 (1977).
[21] J. C. Fuggle, P. Bennett, F. U. Hillebrecht, A. Lenselink, and G. A. Sawatzky, Phys. Rev. Lett. **49**, 1787 (1982).
[22] H. Eskes, G. A. Sawatzky, and L. F. Feiner, Physica C **160**, 424 (1989).
[23] J. C. Slater and G. F. Koster, Phys. Rev. **94**, 1498 (1954).
[24] L. H. Tjeng, J. van Elp, P. Kuiper, and G. A. Sawatzky (unpublished).
[25] *Memory Function Approaches to Stochastic Problems in Condensed Matter,* Vol. 62 of *Wiley Series on Advances in Chemical Physics,* edited by M. W. Evans, P. Grigolini, and G. Pastori Parravicini (Wiley, New York, 1985).
[26] M. R. Thuler, R. L. Benbow, and Z. Hurych, Phys. Rev. B **26**, 669 (1982).
[27] S. Maekawa, J. Inoue, and T. Tohyama, in Ref. 16, p. 66.
[28] J. F. Annett, R. M. Martin, A. K. McMahan, and S. Satpathy, Phys. Rev. B **40**, 2620 (1989).

[29]E. B. Stechel and D. R. Jennison, Phys. Rev. B **38**, 4632 (1988).
[30]J. Ghijsen, L. H. Tjeng, H. Eskes, G. A. Sawatzky, and R. L. Johnson, Phys. Rev. B **42**, 2268 (1990).
[31]F. C. Zhang and T. M. Rice, Phys. Rev. B **37**, 3759 (1988).
[32]M. S. Hybertsen, E. B. Stechel, M. Schlüter, and D. R. Jennison, Phys. Rev. B **41**, 11 068 (1990); M. Schlüter (unpublished).
[33]H. Fukuyama and H. Matsukawa, in Ref. 16, p. 45.
[34]J. Zaanen, Ph.D. thesis, University of Groningen, 1986 (unpublished).
[35]J. Ghijsen, L. H. Tjeng, J. van Elp, H. Eskes, J. Westerink, G. A. Sawatzky, and M. T. Czyzyk, Phys. Rev. B **398**, 11 322 (1988).
[36]N. B. Brookes, A. J. Viescas, P. D. Johnson, J. P. Remeika, A. S. Cooper, and N. V. Smith, Phys. Rev. B **39**, 2736 (1989).
[37]T. J. Wagener *et al.*, Phys. Rev. B **39**, 2928 (1989); **41**, 4201 (1990).
[38]G. van der Laan, C. Westra, C. Haas, and G. A. Sawatzky, Phys. Rev. B **23**, 4369 (1981).
[39]F. al Shamma and J. C. Fuggle, Physica C **169**, 325 (1990); J. C. Fuggle, J. Fink, and N. Nücker, in *Towards the Theoretical Understanding of High $T_c$ Superconductors,* Proceedings of the Adriatico Research Conference, Trieste, Italy, 1988, edited by S. Lundqvist, E. Tosatti, M. P. Tosi, and Yu Lu (World Scientific, Singapore, 1988), p. 649.
[40]For example, T. Takahashi *et al.*, Phys. Rev. B **37**, 9788 (1988).
[41]G. Wendin, Phys. Scr. T **27**, 31 (1989).
[42]P. Kuiper, G. Kruizinga, J. Ghijsen, G. A. Sawatzky, and H. Verweij, Phys. Rev. Lett. **62**, 221 (1989).
[43]F. D. M. Haldane and P. W. Anderson, Phys. Rev. B **13**, 2553 (1976).